

STUDY ON STRESS-STRAIN RELATIONS FOR WELD RESIDUAL STRESS SIMULATION OF TYPE 316L STAINLESS STEEL ON BASIS OF NONLINEAR HARDENING LAW

Nobuyoshi Yanagida¹

¹ Chief Researcher, Hitachi, Ltd., Ibaraki, Japan (nobuyoshi.yanagida.fw@hitachi.com)

ABSTRACT

Thermal elastic plastic analysis is widely used to estimate weld residual stress. Temperature-dependent stress-strain relation is an important mechanical property. In this study, stress-strain curves from room temperature to high temperature were measured and fitted with high accuracy on the basis of the nonlinear hardening law for use in thermal elastic plastic analysis. The tested material was type 316L stainless steel. Tensile tests were performed at temperatures of 20, 100, 200, 400, 600, 800 and 950°C. The tensile load was applied at a constant strain rate until the tensile test specimen ruptured. To use the stress-strain curves obtained from the high-temperature tensile test for weld residual stress simulation by thermal elastic plastic analysis, the relationship between plastic strain and stress after the stress exceeds the yield stress needs to be expressed in a mathematical expression. The stress-strain curve at each temperature was fitted with an exponential function on the basis of the nonlinear hardening law. The constants for the fitting equation between plastic strain and stress were determined at each measurement temperature. By using the determined constants, the stress-strain relations required for thermal elastic plastic analysis were defined.

INTRODUCTION

To estimate the reliability of welded structures, residual stress profiles need to be predicted. To determine the residual stress profiles, thermal elastic plastic analysis has been widely used (Ogawa, 2008, Yanagida et al. 2009). The stress-strain history in the welding process in the structure is complex. For example, during the heat input process when a structure is being welded, the compressive yielding follows the compressive stress around the heat input region of the structure. In addition, during the cooling process after heat input, the compressive plastic strain generated by the yielding generates tensile stress. Both processes, i.e., the compressive yielding and subsequent compressive plastic strain that occur during the heat input process and the tensile stress that occurs during the cooling process, are repeated during the welding process.

To accurately analyze the residual stress profiles in such welded structures, the stress-strain relation (constitutive law) from room temperature to melting temperature is important. To determine the stress-strain relation for the thermal elastic plastic analysis, tensile tests of austenitic stainless steel were performed from room temperature to 800°C (Yanagida, 2008). Stress-strain curves were measured until the strain reached 0.1. The material properties were determined on the basis of the stress-strain curves up to 0.1 strain. However, for austenitic stainless steel such as type 316L, the strain at which the tensile test specimen ruptures is in the range of 0.3 to 0.6, and the tensile strength is indicated just before this point. Therefore, the stress-strain curve as material strength data should measure the relationship between stress and strain until the tensile test specimen ruptures.

When the measured results of the stress-strain relation are applied to thermal elastic plastic analysis using the finite element method, they need to be organized as input data for the strength properties of the material. In general-purpose analysis codes, for example, stress-strain curves that exhibit nonlinear behavior may be approximated by multilinear approximation as input data. On the other hand, in some cases, a stress-strain curve is fitted by a nonlinear equation and the necessary constants are used as input data. In this study,

nonlinear equation fitting of measured stress-strain curves was performed. The fitting method and the constants determined were validated, and the fitting results and measured results were compared.

TESTED MATERIAL AND TENSILE TEST SPECIMEN

The material used for the test was type 316L austenitic stainless steel. The material composition listed on the mill sheet is shown in table 1. The material was held at 1060°C for 2 minutes as a solution heat treatment, followed by a rapid cooling by water quenching. Tensile test specimens were taken from a pipe of the material with an outer diameter of 268 mm and a thickness of 15 mm, with the direction of the center axis of the tensile test specimen coinciding with the direction of the center axis of the pipe, and the center axis of the tensile test specimen was centered in the thickness of the pipe.

The tensile test specimens with a parallel section diameter of 6 mm were fabricated. Two protrusions with a triangular cross section were formed on the parallel section. The distance between the protrusions was 30 mm. The displacement between the protrusions was measured with a differential displacement transducer during the tensile test, and strain was determined by dividing the measured displacement by the initial distance between the protrusions. The tensile load on the tensile test specimen was also measured by a load cell, and stress was determined by dividing the measured load by the initial cross-sectional area of the tensile test specimen.

Table 1: Listed value on the mill sheet of the tested type 316L.

Alloying elements	C	Si	Mn	P	S	Cr	Ni	Mo	B	N	C+N
wt%	0.015	0.47	1.41	0.019	0.001	18.00	11.56	2.11	0.015	0.11	0.12

HIGH-TEMPERATURE TENSILE TEST CONDITIONS

The high-temperature stress-strain relations required for thermal elastic plastic analysis were measured by high temperature tensile tests on tensile test specimens taken from the material. The test conditions and test procedures are described below.

When thermal elastic plastic analysis is used to predict weld residual stress, the stress-strain relation is required in the temperature range from room temperature, where the material property has stiffness, to high temperature, where the material has little stiffness. Therefore, high temperature tensile tests were conducted at seven test temperatures ranging from room temperature to 950°C. The tensile test specimens were heated by electric heaters installed around the specimens.

In the tensile tests, both ends of the tensile test specimens are fixed to the crosshead of the tensile testing machine, and the displacement speed of the crosshead is controlled by a controller to achieve the strain rate of the test conditions. In the tensile tests, the displacement was applied to the crosshead when the tensile specimen reached the temperature of the test conditions and maintained a constant temperature. The test conditions are listed in table 2. At test temperatures below 600°C, the strain rate was set to 0.003 / min; above 800°C, the strain rate was set to 0.06 / min due to significant creep. In the tensile test, the stress-strain curve was measured until the specimen ruptured. The load applied to the tensile specimen was measured by a load cell, and the stress was determined by dividing the measured load by the initial cross-sectional area of the tensile specimen.

Table 2: Strain rate conditions of the high-temperature tensile tests.

Test temperature (°C)	20	100	200	400	600	800	950
Strain rate (1/min)	0.003	0.003	0.003	0.003	0.003	0.06	0.06

MEASUREMENT RESULTS

High-temperature tensile tests were conducted under the test conditions listed in table 2. Figure 1 shows the stress-strain curves until the tensile specimen ruptured. Figure 2 shows the strain range from 0 to 0.020, indicating the elastic range.

In the measurement results from 20 to 600°C, the stress increases after yielding until the strain value reaches about 0.3 to 0.6, and after the tensile strength is reached, the stress decreases rapidly to rupture. The measurement at 600°C shows sawtooth stress fluctuations. Such stress fluctuations on the stress-strain curve are a phenomenon known as serration and are caused by the movement of dislocations in the crystal and their interaction with solute atoms. At 800 and 950°C, after yielding, the strain increases as the stress decreases. Creep strain occurs when steel materials reach high temperatures. Therefore, the strains at 800 and 950°C are affected by creep.

The strength properties obtained from the measurements are shown in table 3: 0.2% proof stress and tensile strength decrease monotonically as test temperature increases. Elongation shows a significant increase at 800 and 950°C.

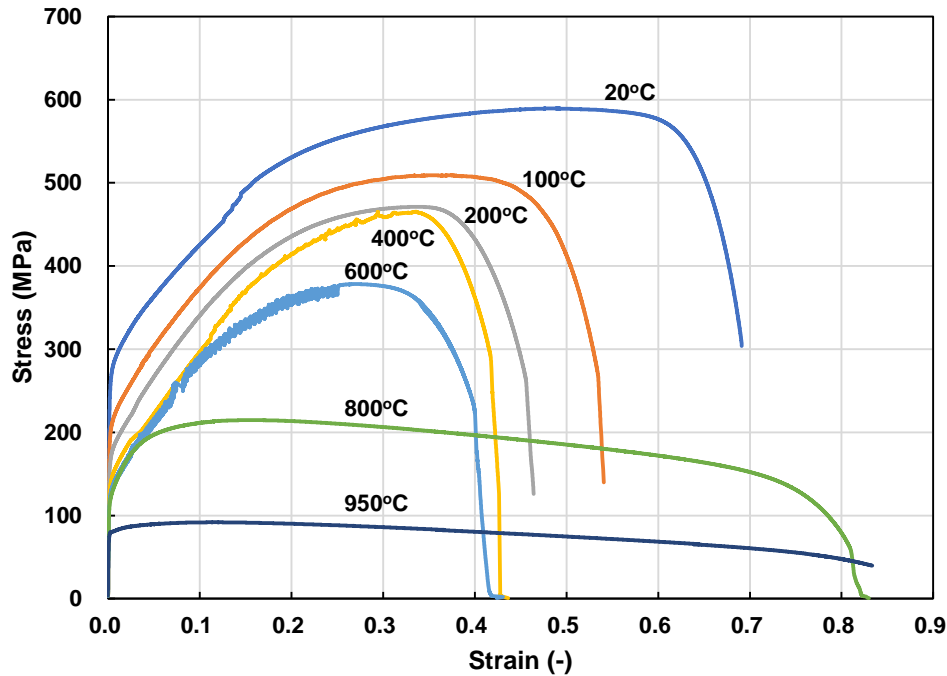


Figure 1. Stress-strain curves from room temperature to 950°C.

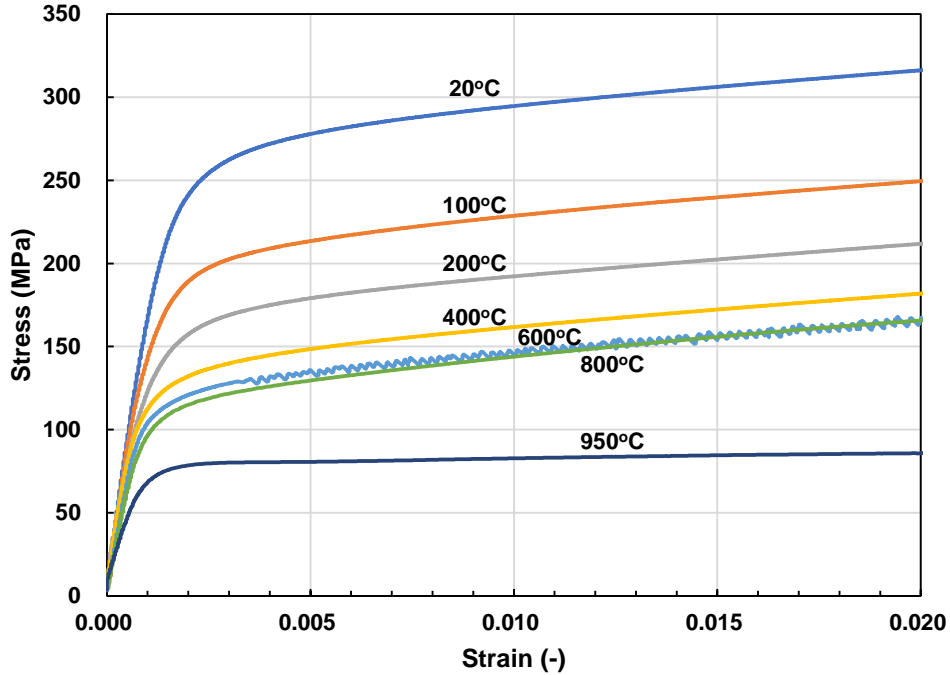


Figure 2. Enlarged view of the stress-strain curves up to 0.020 strain.

Table 3: High-temperature tensile test results.

Temperature (°C)	Young's modulus, E (MPa)	0.2% proof stress, σ_y (MPa)	Tensile strength, σ_B (MPa)	Elongation (%)	Reduction of area (%)
20	190,400	267	589	73.0	86
100	183,400	203	509	54.0	87
200	176,800	169	471	46.5	84
400	161,200	139	465	44.5	79
600	144,900	127	378	45.0	78
800	123,500	122	215	84.5	92
950	92,600	80	92	99.5	99

FITTING BY NONLINEAR HARDENING LAW

To use stress-strain curves obtained from tensile tests to predict weld residual stress by thermal elastic plastic analysis, the relation between plastic strain and stress after the stress exceeds the yield stress needs to be expressed in a mathematical expression. In this study, the stress-strain relation was fitted by a nonlinear hardening law using an exponential function.

The nonlinear hardening law is a model of defining the relation between stress and plastic strain after yielding using an exponential function. It is implemented as an optional function in a general-purpose analysis code and defines the relation between plastic strain and stress using equation (1) or (2).

$$\text{Nonlinear kinematic hardening: } \sigma = \sigma_y + \frac{C}{\gamma} \left(1 - e^{-\gamma \varepsilon^{pl}}\right) \quad (1)$$

$$\text{Nonlinear isotropic hardening: } \sigma = \sigma_y + Q_\infty \left(1 - e^{-b \varepsilon^{pl}}\right) \quad (2)$$

In the case of the kinematic hardening law, stress increases as the center of the yield surface shifts as plastic deformation progresses. In the case of the isotropic hardening law, the stress increases as the size of the yield surface expands as plastic deformation progresses.

In equations (1) and (2), σ_y is the initial yield stress, C and γ are the constants for the kinematic hardening law and Q_∞ and b are the constants for the isotropic hardening law. The constants in equations (1) and (2) are discussed here. The relation between stress σ and plastic strain ε^{pl} can be approximated by equation (3).

$$\sigma = \sigma_y + A \left(1 - e^{-k \varepsilon^{pl}}\right) \quad (3)$$

In equation (3), A and k are constants. Once these values are determined, by comparing equations (1) and (3), the kinematic hardening constants, C and γ , in equation (1), can be determined as in equation (4). Also, by comparing equations (2) and (3), the isotropic hardening constants, Q_∞ and b , in equation (2), can be determined as in equation (5).

$$\text{Nonlinear kinematic hardening: } C = Ak, \quad \gamma = k \quad (4)$$

$$\text{Nonlinear isotropic hardening: } Q_\infty = A, \quad b = k \quad (5)$$

As described above, the fitting of the stress-plastic strain curve based on equation (3) makes it possible to establish the stress-strain relation required for thermal elastic plastic analysis. The fitting procedure is described below, using the measured stress-strain curve of 20°C shown in figure 1 as an example. First, Young's modulus E is determined. Young's modulus E can be calculated as the slope of the stress-strain relationship immediately after the start of loading, as shown in figure 2, where stress is linearly related to strain. Next, the relationship between stress and plastic strain ε^{pl} is determined. The plastic strain ε^{pl} can be obtained from the stress σ in the test results, the elastic plastic strain ε ($=\varepsilon^{el} + \varepsilon^{pl}$) and the Young's modulus E obtained above, as follows.

$$\varepsilon^{pl} = \varepsilon - \frac{\sigma}{E} \quad (6)$$

The relationship between the plastic strain ε^{pl} and stress σ calculated by equation (6) is shown in figure 3. The stress at a plastic strain value of 0.002 calculated from equation (6) is the 0.2% proof stress, which was measured to be 267 MPa. In this study, the 0.2% proof stress was used as the value of the initial yield stress σ_y . In figure 3, σ_y is written as 267 MPa, but strictly speaking, 267 MPa is the value when the plastic strain is 0.002.

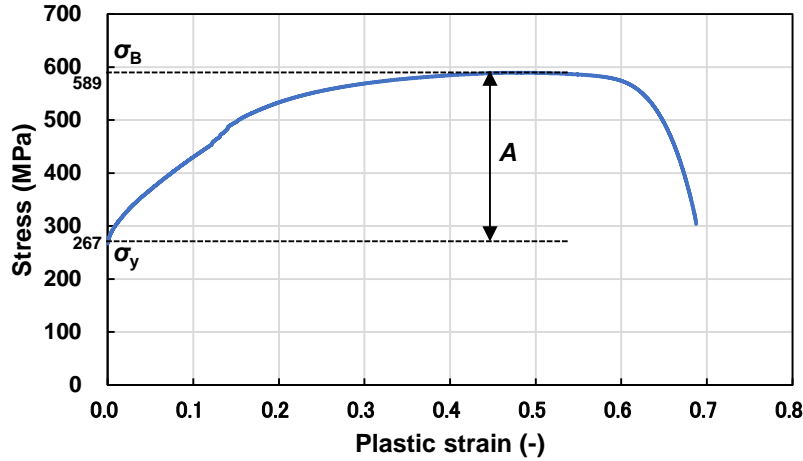


Figure 3. Stress versus plastic strain relation at 20°C.

To fit the stress-plastic strain relation shown in figure 3 in equation (3), A and k in equation (3) need to be found. On the basis of equation (3), the following relation is obtained in equation (7).

$$\sigma = \sigma_y \text{ when } \varepsilon^{pl} = 0 \quad (7)$$

Furthermore, on the basis of equation (3), the following relationship can be also obtained in equation (8). Note that, based on figure 3, $\sigma_y + A$ is σ_B .

$$\sigma \rightarrow \sigma_y + A (= \sigma_B) \text{ when } \varepsilon^{pl} \rightarrow \infty \quad (8)$$

Therefore, A is calculated by equation (9).

$$A = \sigma_B - \sigma_y \quad (9)$$

Equation (3) can also be rewritten as in equation (10).

$$Ae^{-k\varepsilon^{pl}} = A - \sigma + \sigma_y \quad (10)$$

Substituting equation (9) into equation (10), taking the logarithm of both sides and rearranging, gives equation (11).

$$k\varepsilon^{pl} = -\ln \frac{\sigma_B - \sigma}{\sigma_B - \sigma_y} \quad (11)$$

That is, the relationship between the plastic strain ε^{pl} and the parameter $-\ln \frac{\sigma_B - \sigma}{\sigma_B - \sigma_y}$ calculated from the stresses σ , σ_B , and σ_y can be determined, and the constant k to be multiplied by the plastic strain ε^{pl} can be determined as its slope. The right-hand side of equation (11) was calculated by using the data on the relation between stress and plastic strain shown in figure 3. The results of the calculation are shown in figure 4. The slope of the graph is k , and the value is 8.596.

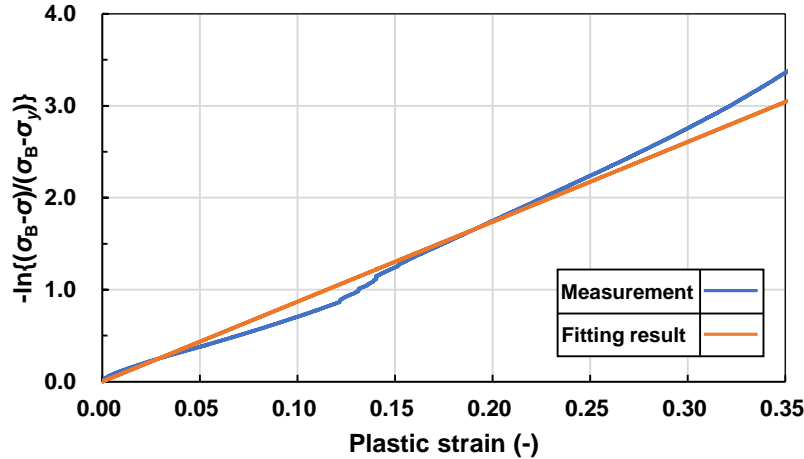


Figure 4. Relationship between plastic strain and a parameter.

The stress-strain curve calculated by substituting the values obtained above into equation (3) is shown in figure 5, which shows that the yield stress σ_y to the tensile strength σ_B can be calculated accurately. In the measurement results shown in figure 5, after the stress reaches the tensile strength σ_B , the stress decreases and leads to rupture. On the other hand, the calculation results based on equation (3) are assumed to be constant after the tensile strength σ_B is reached. In the stress-strain relation shown in figure 5, the strain range from 0 to 0.020 is extended and shown in figure 6. The measurement result shows that the stress-strain curve starts to bend gradually after the yield point, and the increase in strain with increasing stress becomes larger. In the fitting result, the yield stress was assumed to be 0.2% proof stress. Therefore, in the fitting result, the stress increases linearly up to 0.2% proof stress of the measurement results. After the stress reaches the 0.2% proof stress of the measurement results, plastic deforms, and the strain increases significantly.

The measured stress-strain curves at test temperatures other than 20°C were also fitted using the above procedure. The values of the constants Young's modulus E , initial yield stress σ_y , and the constants A and k in the fitting are shown in table 4. The stress-strain curves calculated by using the constants listed in table 4 are shown in figure 7, along with the measurement results. The stress-strain curves for each test temperature show that the measured results can be fitted by two variables: A and k . By applying A and k to equations (4) or (5), the material constants for the nonlinear kinematic hardening law or the nonlinear isotropic hardening law can be obtained.

Note that for the test temperature of 20°C shown in figure 5 and for the test temperatures between 100 and 400°C shown in figure 7(a) to (c), there is a difference between the measured and fitted results in the vicinity of strain values of 0.2 to 0.4. This difference is dependent on the value of k . The difference is about 20 MPa smaller in the fitted result for stresses of about 400 to 500 MPa.

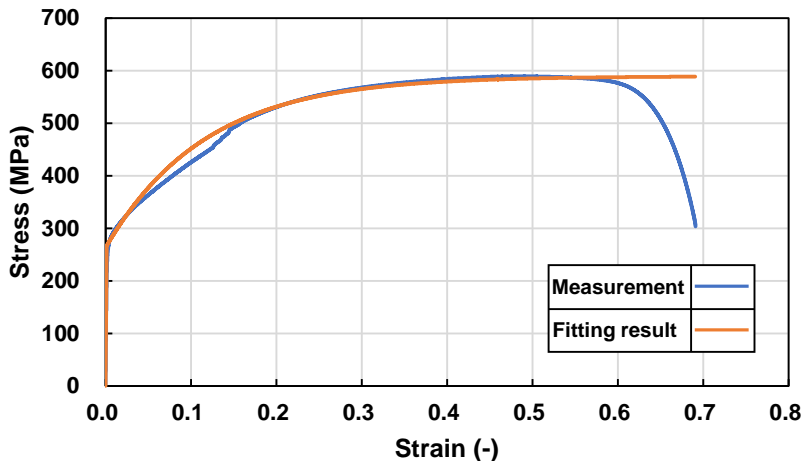


Figure 5. Comparison of measurement data and fitting result at room temperature 20°C.

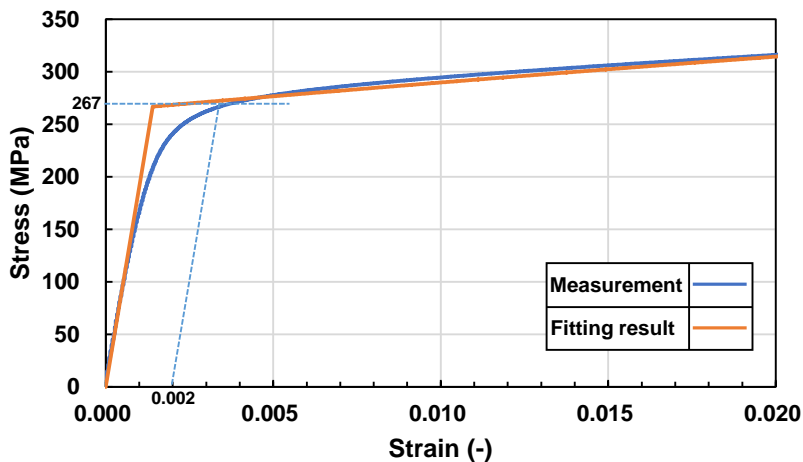
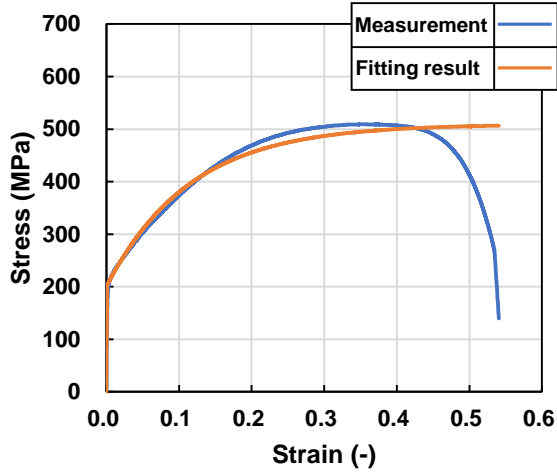


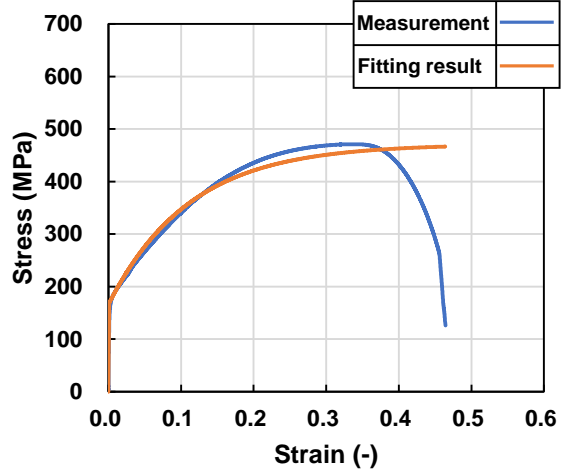
Figure 6. Enlarged view of the stress-strain curve up to 0.020 strain at room temperature 20°C.

Table 4: Material constants for the fitting equation.

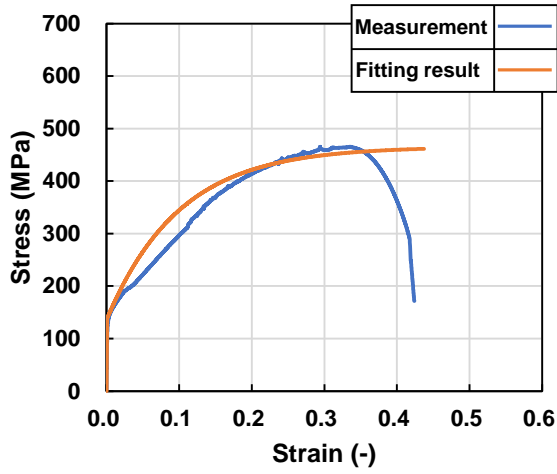
Temperature (°C)	Young's modulus (MPa)	Yield stress (MPa)	A (MPa)	k (-)
20	190,400	267	322	8.596
100	183,400	203	306	8.799
200	176,800	169	303	9.103
400	161,200	139	326	10.16
600	144,900	127	251	10.13
800	123,500	122	93	35.19
950	92,600	80	12	35.75



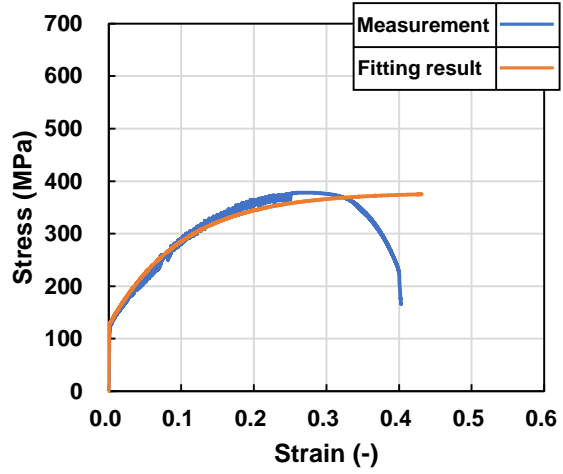
(a) 100°C



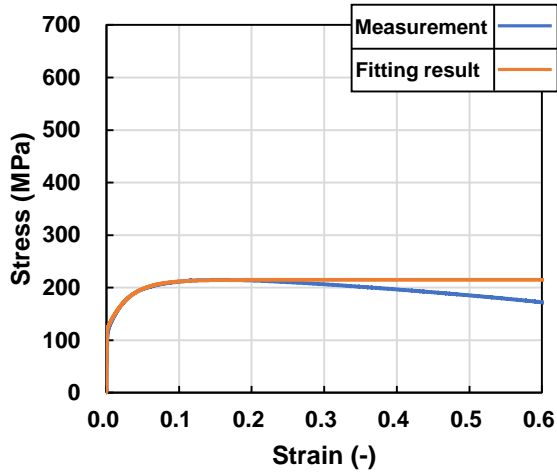
(b) 200°C



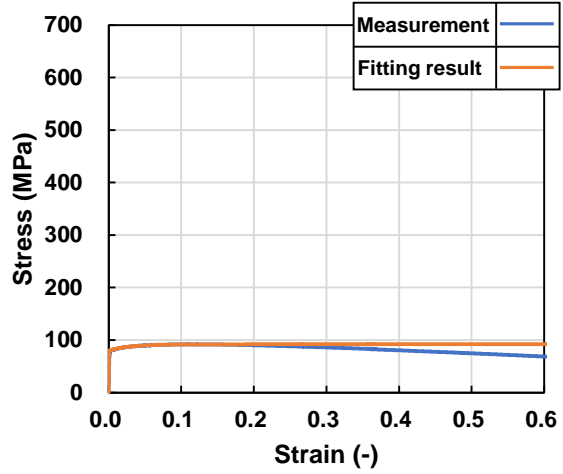
(c) 400°C



(d) 600°C



(e) 800°C



(f) 950°C

Figure 7. Comparison of measurement data and fitting result.

Table 5 lists the material properties of the nonlinear kinematic hardening law shown in equation (4) and the nonlinear isotropic hardening law shown in equation (5), calculated from the constants in equation (3) shown in table 4. By using these values, stress-strain curves can be set up from room temperature to 950°C. In this study, the measured stress-strain curves were approximated by the nonlinear kinematic hardening law or the nonlinear isotropic hardening law as described above. On the other hand, type 316L is known to actually undergo combined hardening with both the kinematic hardening and the isotropic hardening behaviors. The approximation of the stress-strain relation by the combined hardening law should be investigated in the future through additional material tests or sensitivity analysis of weld residual stresses by thermal elastic plastic analysis with the ratio of the kinematic hardening and the isotropic hardening as a parameter.

Table 5: Material constants for the nonlinear hardening law.

Temperature (°C)	Kinematic hardening law		Isotropic hardening law	
	C (MPa)	γ (-)	Q_{∞} (MPa)	b (-)
20	2768	8.596	322	8.596
100	2692	8.799	306	8.799
200	2758	9.103	303	9.103
400	3312	10.16	326	10.16
600	2543	10.13	251	10.13
800	3273	35.19	93	35.19
950	429	35.75	12	35.75

CONCLUSION

Stress-strain curves of austenitic stainless steel type 316L were measured from room temperature to 950°C by tensile testing until the tensile test specimen ruptured to develop material property data for the stress-strain relation necessary to analyze weld residual stress by thermal elastic plastic analysis. Constants were determined on the basis of exponential fitting of the measured stress-strain curves. It was found that the measurement results could be fitted with high accuracy. Furthermore, the material properties required for setting the stress-strain curves by the nonlinear kinematic hardening law and nonlinear isotropic hardening law were determined. The determined material properties enable the stress-strain relation to be set on the basis of the kinematic hardening law or the isotropic hardening law for austenitic stainless steel type 316L.

REFERENCES

- Ogawa, K., Yanagida, N. and Saito, K. (2008). "Residual Stress Prediction for Non-Axisymmetric Vessel Penetration Welds," *Proceedings of ASME Pressure Vessels and Piping Conference*, PVP2008-61321, July 27-31, 2008, Chicago, Illinois, USA.
- Yanagida, N., Ogawa, K., Saito, K. and Kingston, E. (2009). "Study on Residual-Stress Redistributions during the Process of Manufacture of a Vessel Penetration Set-on Joint," *Proceedings of ASME Pressure Vessels and Piping Conference*, PVP2009-77408, July 26-30, 2009, Prague, Czech Republic.
- Yanagida, N. (2008). "Study on Stress-Strain Relation for Type 316L Stainless Steel Using Mixed Hardening Law," *Proceedings of ASME Pressure Vessels and Piping Conference*, PVP2008-61404, July 27-31, 2008, Chicago, Illinois, USA.